Available online at www.sciencedirect.com
SCIENCE DIRECT®
Optics Communications 234 (2004) 193–202
OPTICS COMMUNICATIONS
www.elsevier.com/locate/optcom

Continuous wave-controlled shape and chirp oscillations of optical solitons

Yannis Kominis, Kyriakos Hizanidis *

Department of Electrical and Computer Engineering, National Technical University of Athens, 9 Iroon Polytexniou, 15773 Athens, Greece

Received 3 July 2003; received in revised form 3 February 2004; accepted 12 February 2004

Abstract

Interactions between solitons and continuous waves (CW) are studied in terms of a perturbation method and systematic numerical simulations as well. The critical dependence of the interactions on the initial phase difference between the pulse and the CW is shown to result in two distinct types of evolution under propagation. Pulse shape and chirp oscillations occur for specific configurations of pulse and CW initial amplitudes and phase difference, while pulse destruction and splitting occurs for other possible configurations. The effect of modulational instability, emerging from the interactions, is also considered.

PACS: 060.4510; 060.5530; 190.5330; 060.4230

Keywords: Solitons; Chirp; Modulation

1. Introduction

Optical soliton stability and interactions under long distance propagation have been considered in great extent in the context of potential applications in high bit-rate communication systems. Their remarkable stability and persistence of propagation characteristics under mutual interactions and collisions have made them good candidates for information carriers and have lead to the proposal of soliton communication systems [1]. However, such a communication system, in order to be technologically realistic and efficient, should include devices and methods of controlling soliton pulse propagation characteristics in the optical layer, meeting the demand for all-optical control which includes amplification, reshaping, routing, filtering and wavelength conversion. This paper investigates the interactions between solitons and continuous waves (CW) in order to establish the way that certain soliton characteristics are affected by the presence of intentionally injected CW.

Soliton interactions with CW have arised as an undesirable feature in high bit-rate communication systems where some residual CW background

* Corresponding author. Tel.: +30-210-772-3685; fax: +30-210-772-3513.
E-mail address: kyriakos@central.ntua.gr (K. Hizanidis).

0030-4018/$ - see front matter © 2004 Elsevier B.V. All rights reserved.
doi:10.1016/j.optcom.2004.02.035

might appear due to the generation or amplification process [2]. On the other hand the injection of a CW with the same frequency and phase as the soliton has been proposed as a reshaping and amplification method [3], and the intentional mixing of a soliton with a CW background has been suggested for detecting the phase of the first [4]. Also, amplitude variations of accompanying quasi-continuous radiation have been proved capable of providing a mechanism for controlling the reconstruction period of femtosecond soliton pulses in the presence of third-order dispersion [8].

The aforementioned applications of such interactions have risen the interest for exact solutions of the non-linear Schröedinger (NLS) equation capable of describing their features [4–6]. These solutions are obtained under the strong assumption that the amplitude of the CW background remains constant under propagation and describe a breather-like bound solitary wave on the CW background for the special case in which the pulse and CW are $\pi/2$ out-of-phase. However, the background field is unstable relative to perturbation as it is widely known due to the phenomenon of modulational instability (MI) of the NLS [7]; thus the whole solutions must be viewed as unstable, and under certain circumstances the soliton part can be hidden in "noise" created by this instability after long distance propagation.

Other approaches have also been adopted including: perturbation method for solving the associated Zakharov–Shabat eigenvalue problem [3] for small amplitude CW, direct perturbation for the case of purely radiative perturbations [9], and variational methods utilizing an ansatz restricted to out-of-phase interactions between the soliton and the CW [10,11].

In the present work an inverse scattering transform-based perturbation method is applied, resulting in a one-degree of freedom Hamiltonian dynamical system for the pulse width/amplitude evolution under propagation. The latter gives quantitative information about pulse shape oscillations for small CW amplitudes. Moreover, the qualitative information about distinct types of pulse evolution dynamics and their critical dependence on the initial phase difference between the pulse and the CW, apply to even larger values of CW amplitude. Also, a systematic numerical investigation, utilizing direct simulations of the original system, is applied for comparison with the aforementioned results, extending our study for larger values of CW amplitudes and also for including additional features of the interactions such as pulse chirping and modulational instability. Finally, a two-dimensional (2D) spectral analysis is utilized as a tool for the summarized visualization of all spectral components of the interactions in the context of a generalized dispersion relation.

2. Model and perturbation method

The equation governing pulse propagation in a non-linear optical fiber in the anomalous dispersion regime is the NLS equation, which can be written in non-dimensional form as:

$$\mathrm{i}\frac{\partial u}{\partial Z}+\frac{1}{2}\frac{\partial^2 u}{\partial T^2}+|u|^2u=0, \tag{1}$$

where u is the complex-valued envelope of the pulse, Z is the normalized propagation distance along the fiber and T is the normalized time measured in a coordinate system travelling with the group velocity of a pulse [1]. The NLS equation has the well-known soliton solution

$$u_{\mathrm{s}}(T,Z)=n\,\mathrm{sech}(nT)\exp(\mathrm{i}\sigma),\quad \sigma=\frac{n^2}{2}Z \tag{2}$$

with n,σ being real numbers, obtained by the inverse scattering transform (IST) method which shows that a general initial condition $u(T,0)$ evolves into a fixed number of solitons plus decaying dispersive radiation. However, while the asymptotic state of the solution can be easily obtained, the transient evolution dynamics of the initial condition until reaching the final state is quite difficult to be determined in the context of the IST method. This is because this state is mostly driven by interactions between the emerging solitons and the radiation which is very difficult to determine from the corresponding integral equation of the IST method. In order to overcome these difficulties we adopt the following perturbation approach.

Since we are interested in the evolution of the superposition of a bright soliton pulse and a CW the solution of the NLS equation can be written

$$u = u_s + u_{cw}, \tag{3}$$

where u_s is the bright soliton solution of the NLS Eq. (2) and $u_{cw} = \alpha \exp(i\phi)$ with α and ϕ denoting the amplitude and the phase of the CW, respectively. Substitution of (3) in the NLS equation leads to a non-linear term of the form $|u|^2 u = |u_s|^2 u_s + u_s^2 u_{cw}^\star + 2|u_s|^2 u_{cw} + 2u_s|u_{cw}|^2 + u_{cw}^2 u_s^\star + |u_{cw}|^2 u_{cw}$. After omitting terms that are second and third order in $|u_{cw}|$ a perturbed NLS equation is obtained

$$i\frac{\partial u_s}{\partial Z} + \frac{1}{2}\frac{\partial^2 u_s}{\partial T^2} + |u_s|^2 u_s = R(u_s, u_{cw}), \tag{4}$$

where $R(u_s, u_{cw}) = u_s^2 u_{cw}^\star z + 2|u_s|^2 u_{cw}$ is the perturbation term modifying the pulse propagation due to the presence of the CW.

The perturbed NLS Eq. (4) is studied according to the IST-based perturbation method [1] which results to a dynamical system for pulse width (amplitude) and phase evolution:

$$\frac{dn}{dZ} = \frac{1}{2}\alpha\pi n^2 \sin(\sigma - \phi), \tag{5}$$

$$\frac{d\sigma}{dZ} = \frac{1}{2}n^2 + \alpha\pi n \cos(\sigma - \phi). \tag{6}$$

The system has a Hamiltonian

$$H = -\frac{n^3}{6} - \frac{\alpha\pi n^2}{2}\cos(\sigma - \phi) \tag{7}$$

which is also an invariant of the motion, since it is not an explicit function of the dynamic variable Z. The solutions of the system can be written in the following form:

$$Z - Z_0 = \pm \int_{n_0}^{n} \frac{6dn}{\sqrt{(3\alpha\pi n^2)^2 - (6H + n^3)^2}}. \tag{8}$$

Instead of considering this complicated form of the solution, we proceed our study with a phase space analysis of system dynamics. The 2D phase space (n, σ) is characterized by the symmetry relations:

$$(n, \sigma + 2\pi) = (n, \sigma), \tag{9}$$

$$(n, \sigma + \pi) = (-n, \sigma), \tag{10}$$

which allow the restriction of the analysis in the area $[0, \infty) \times [0, 2\pi)$. Moreover, the system is invariant under the scaling transformation

$$n \to n/\alpha, \quad Z \to \alpha^2 Z. \tag{11}$$

The trajectories in the phase space are obtained directly as level curves of the Hamiltonian as shown in Fig. 1. The whole line $n = 0$ consists of fixed points of no physical interest and there exists an isolated fixed point in $(n, \sigma) = (2\alpha\pi, \phi + \pi)$. Two regions of qualitatively different types of evolution exist with the separatrix curve given by:

$$n = -3\alpha\pi\cos(\sigma - \phi). \tag{12}$$

Outside the separatrix, the evolution is characterized by variation of the pulse phase σ in the full range $[0, 2\pi)$ (rotation type of oscillation), while inside the separatrix the phase variations are restricted around π (libration type of oscillation). It is remarkable that, since there is no type of soliton-like pulse evolution with restricted phase variation, this "phase trapping" around π is in direct correspondence with pulse destruction as will be also shown by the numerical results. As shown in Fig. 1, for a given initial phase difference $\Delta\phi_0 \equiv \sigma_0 - \phi$, the ratio n/α determines the selection of a particular trajectory which is characterized by a specific period and amplitude of oscillation.

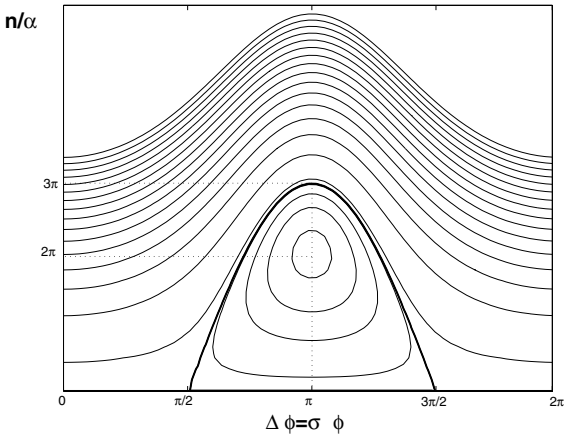

Fig. 1. Phase space of the system.

For the rotation type of oscillation, the increase of the ratio n/α results in more flat trajectories which is reasonable since the pulse is less affected by the much smaller CW. In the limit of very large ratios the trajectories are almost straight lines, the pulse width is almost constant and the spatial frequency of oscillation tends to the value $(1/2)n^2$ of the unperturbed soliton (2) frequency of phase oscillation. Trajectories approaching the separatrix from above have increasing amplitude variation and decreasing frequency of oscillation (for a given α, because according to (11) changing of α results also in period scaling).

3. Numerical results and discussion

In order to compare the results of the previous system with the original model for small CW amplitudes and to extend the range of CW amplitudes to larger values, for which the perturbation approach might be misleading, we utilize a numerical approach based on the beam propagation method (BPM), also known as split step fourier (SSF) to study the evolution of soliton and CW interactions. The numerical method is not subjected to any assumptions and, in contrast with the aforementioned system which provides information only for shape oscillations, it is capable of including other features of the interactions such as pulse chirp oscillations and MI.

3.1. Shape oscillations

The propagation of a soliton pulse (having $n = 1$ for the following analysis) under the presence of a CW of amplitude $\alpha = 0.08,\ 0.16,\ 0.24$ is shown in Figs. 2(a)–(c) and Figs. 3(a)–(c) for a phase difference $\Delta\phi_0 = 0$ and $\Delta\phi_0 = \pi/2$, respectively. The results are in qualitative agreement with the aforementioned model. The pulse amplitude (width) undergoes periodic oscillations. In the first case the initial amplitude is a (local) minimum of the oscillations while in the second case the amplitude takes higher as well as lower values from the initial one, in agreement with the evolution predicted from the phase space analysis (Fig. 1). In both cases the background becomes unstable for larger CW amplitudes and the amplitude of oscillations varies along Z. The case of $\Delta\phi_0 = \pi$ for the same range of amplitudes is shown in Figs. 4(a)–(c). For CW amplitude $\alpha = 0.08$, the initial condition (n, σ) is located outside the

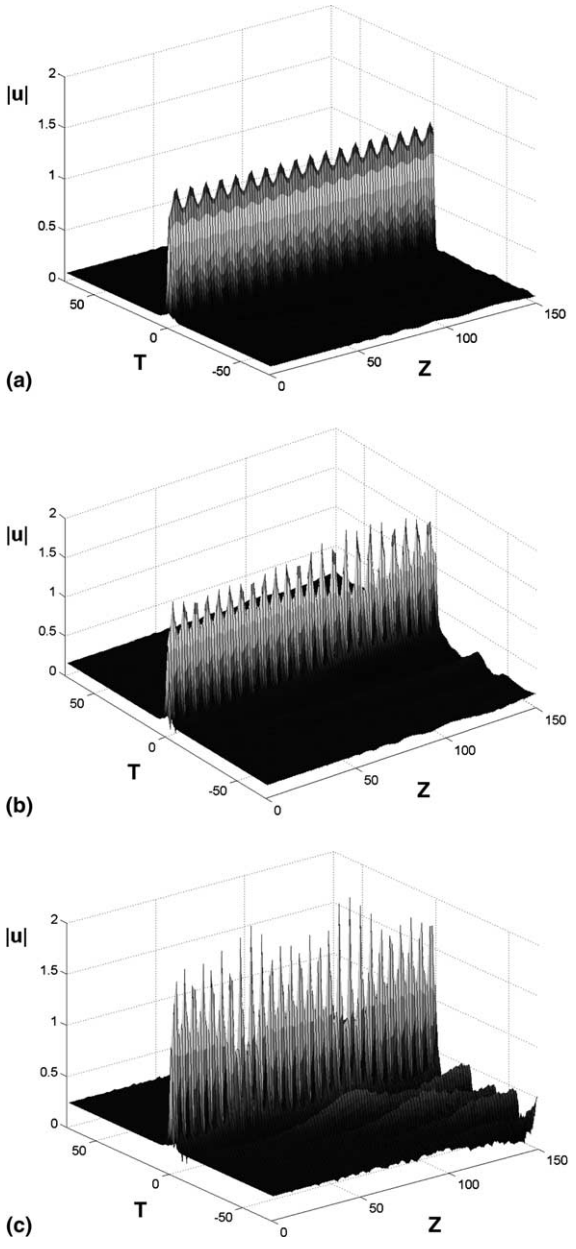

Fig. 2. (a–c) Pulse shape oscillations for a CW with $\phi = 0$ and $\alpha = 0.08,\ 0.16,\ 0.24$, respectively.

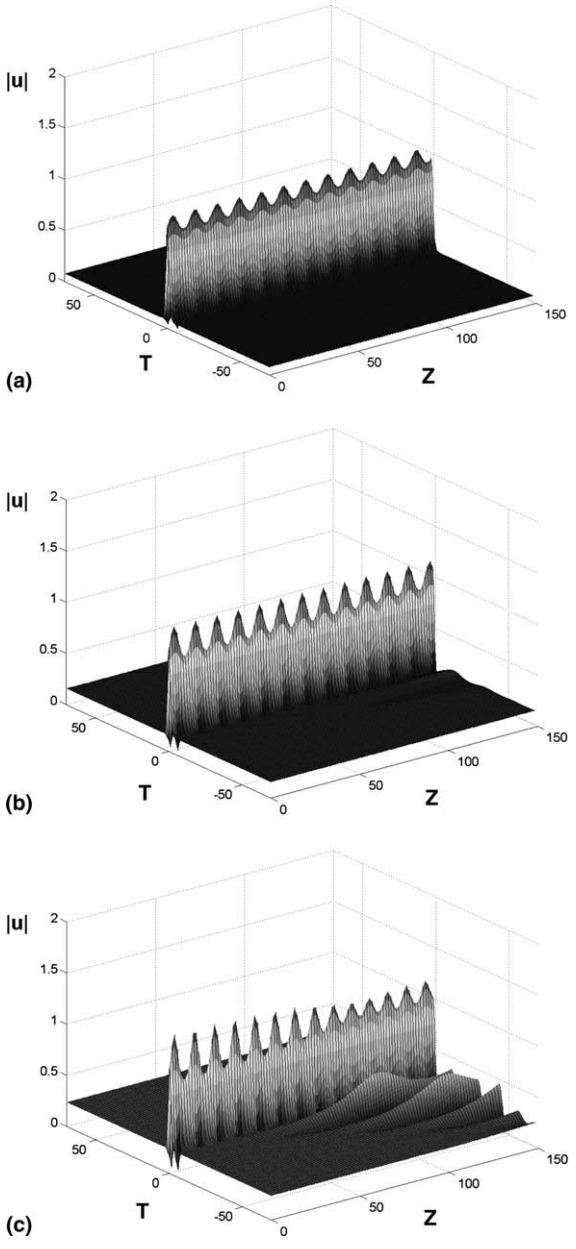

Fig. 3. (a–c) Pulse shape oscillations for a CW with $\phi = \pi/2$ and $\alpha = 0.08,\ 0.16,\ 0.24$, respectively.

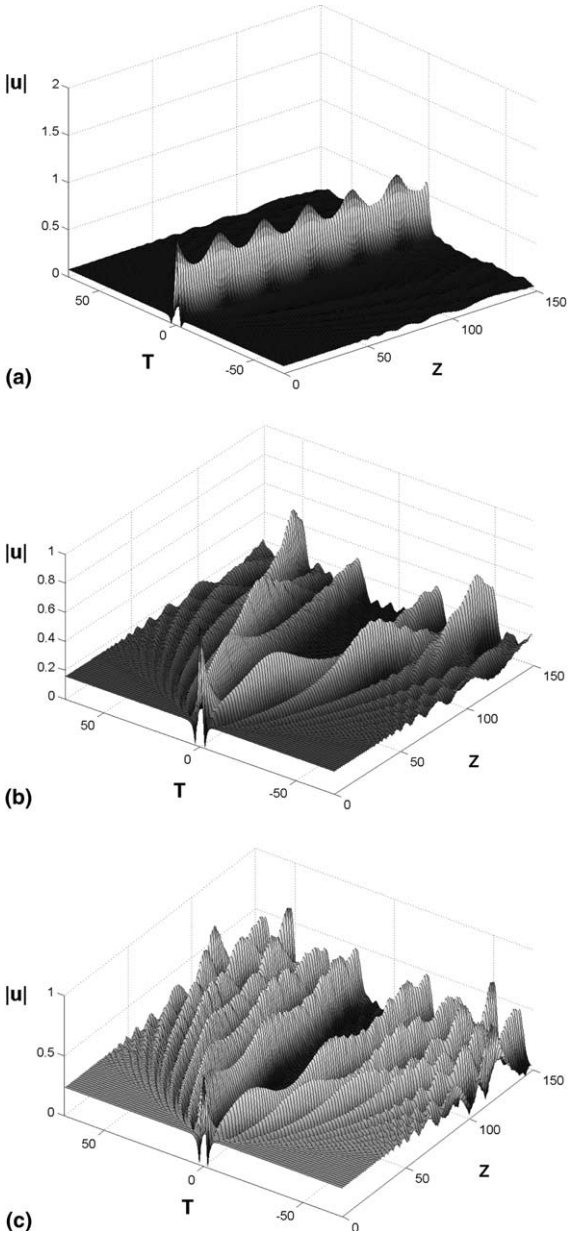

Fig. 4. (a–c) Pulse shape oscillations for a CW with $\phi = \pi$ and $\alpha = 0.08,\ 0.16,\ 0.24$, respectively.

separatrix and the pulse evolution is oscillatory, while for $\alpha = 0.16$ and $\alpha = 0.24$ the initial condition is located close to and below the fixed point, respectively, and pulse destruction (splitting) occurs, confirming the prediction of model (6).

A quantitative comparison of the results is shown in Figs. 5(a)–(c) for CW amplitude $\alpha = 0.08$ and $\Delta\phi_0 = 0, \pi/2, \pi$. A good agreement for the frequency is observed, while the perturbation method predicts larger oscillations for the pulse

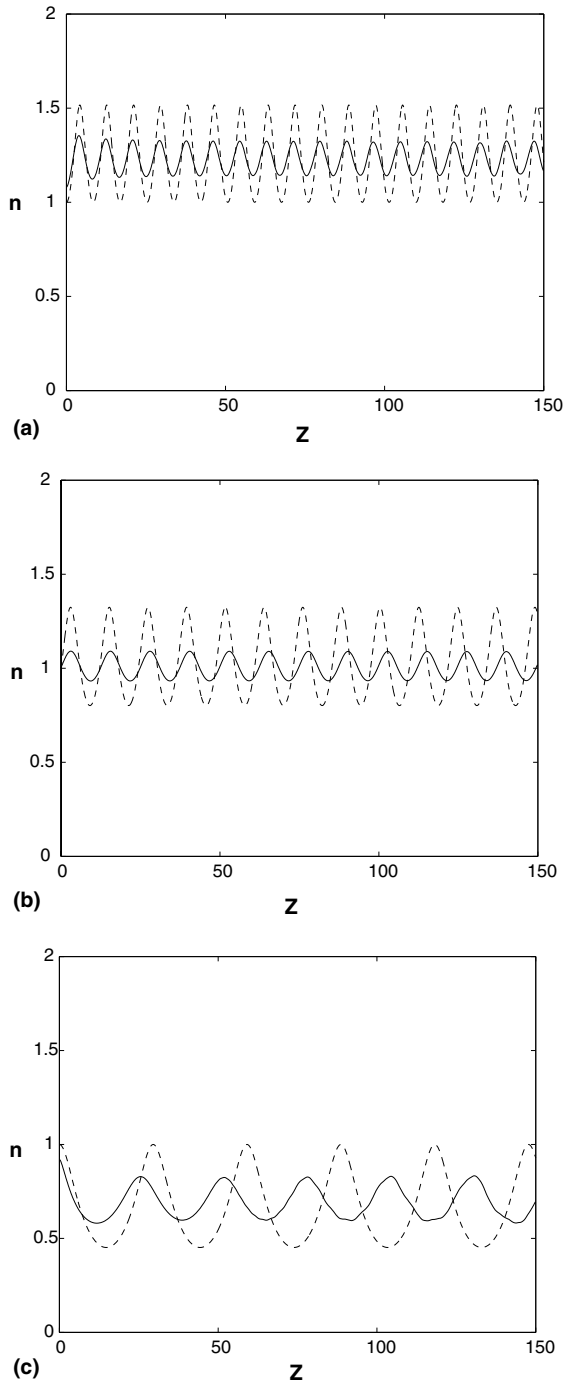

Fig. 5. (a–c) Pulse amplitude oscillations for a CW with $\alpha = 0.08$ and $\phi = 0, \pi/2, \pi$, respectively, as obtained from direct integration of the original model (solid lines) and solution of the model obtained by the perturbation method (dashed lines).

shape than the actual ones. The latter is a result of the drastic reduction of the original infinite-dimensional model to a system of one-degree of freedom. According to this restriction, the interaction is allowed to affect only pulse amplitude since other pulse parameters such as chirp are not included, resulting in overestimation. Model (6) cannot also incorporate the background instability since the perturbation assumes that the amplitude of the CW is fixed. As shown in the numerical solution, energy is being fed into the CW, which

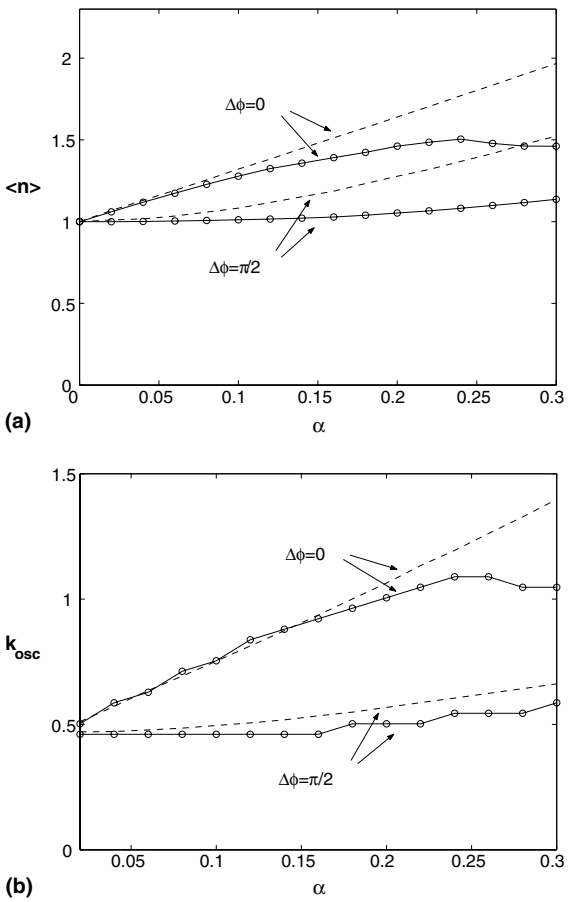

Fig. 6. (a) Shape oscillation mean value versus CW amplitude for $\phi = 0$ and $\phi = \pi/2$ (b) Spatial frequency of shape oscillations versus CW amplitude for $\phi = 0$ and $\phi = \pi/2$ Solid lines with circles and dashed lines, correspond to numerical solutions of the original model and solutions of the perturbation equations, respectively.

evolves under propagation, so that the soliton loses energy.

The mean value of pulse amplitude dependency on the CW amplitude is shown in Fig. 6(a) for the purely oscillatory cases. The drastic effect of the phase difference on this dependency can also be explained in the context of the phase space analysis: for $\Delta\phi_0 = 0$ pulse amplitude is always larger than (or equal to) the initial value, resulting in a mean value much higher than the initial value, while this is not the case for $\Delta\phi_0 = \pi/2$. On the other hand, the increase of the CW amplitude results in the decrease of the ration n/α. However, due to the shape of phase space trajectories, a given variation of n/α does not result in the same capability of selecting a different trajectory for all values of $\Delta\phi$ since the vertical distance of two given trajectories is less for phase difference $\Delta\phi = 0, \pi$ than for $\Delta\phi = \pi/2$.

The spatial frequency of pulse amplitude oscillations k_{osc} as a function of α is shown in Fig. 6(b). For both cases of phase difference the presence of small amplitude CW results in a spatial frequency of 0.5 which is the well-known, analytically predicted frequency of small pulse amplitude oscillations under the presence of small perturbations. As α increases, the two cases are differentiated: while the spatial frequency depends strongly on α when $\Delta\phi_0 = 0$, it remains almost constant (within the precision of the numerical method) for a range of α when $\Delta\phi_0 = \pi/2$. The same arguments as for the mean value can be used to explain this phase dependency. However, although the increase of α results in trajectories approaching the separatrix from above, the spatial frequency of oscillations increases due to the α-dependent scaling transformation of Z (11).

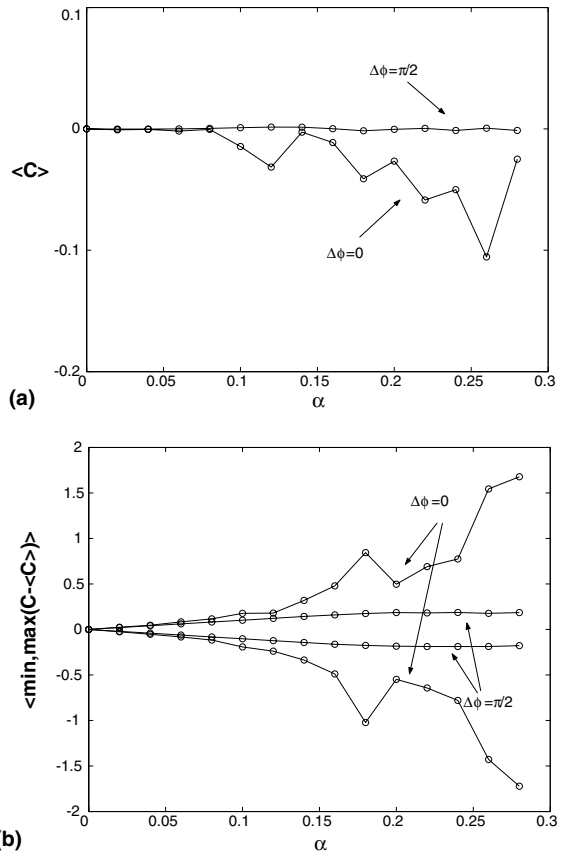

Fig. 7. (a) Chirp oscillation mean value versus CW amplitude for $\phi = 0$ (solid line) and $\phi = \pi/2$ (dashed line). (b) Strength of chirp oscillations measured as the mean maximum and minimum difference of chirp oscillations from the mean value $\langle \max, \min(C - \langle C \rangle) \rangle$ versus CW amplitude for $\phi = 0$ (solid line) and $\phi = \pi/2$ (dashed line).

3.2. Chirp

Interactions between soliton pulses and CW have a significant impact on the pulse phase which

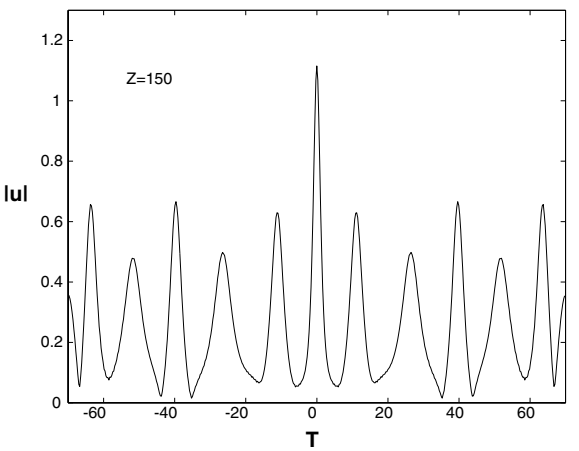

Fig. 8. Manifestation of the modulational instability effect for the case of pulse interaction with a CW having $\alpha = 0.3$ and $\phi = \pi/2$ for $Z = 150$.

is actually perturbed so that the frequency is no longer constant with time T. Time variations of frequency are defined as frequency chirp which is measured by the chirp parameter:

$$C = \frac{1}{2}\frac{\partial^2 \arg(u)}{\partial T^2}\bigg|_{T=0}. \tag{13}$$

In the presence of CW, frequency chirp oscillates as pulse propagates having the same spatial frequency with the aforementioned pulse amplitude oscillations. The mean value and the mean maximum and minimum difference from mean value of these oscillations are shown in Figs. 7(a) and (b), respectively, for phase differences $\Delta\phi_0 = 0, \pi/2$. Independently of $\Delta\phi_0$ the chirp oscillations are symmetric around the mean value, which has a complex dependence on the CW amplitude α for $\Delta\phi_0 = 0$, while being almost independent of α for $\Delta\phi_0 = \pi/2$.

3.3. Modulational instability

The effects of Modulational Instability enter into play as the CW amplitude increases, and manifest themselves as a periodic pulse train having smaller amplitude than the soliton pulse (Figs. 2(c) and 3(c)). These effects result in the reduction of the control capabilities provided by the CW on

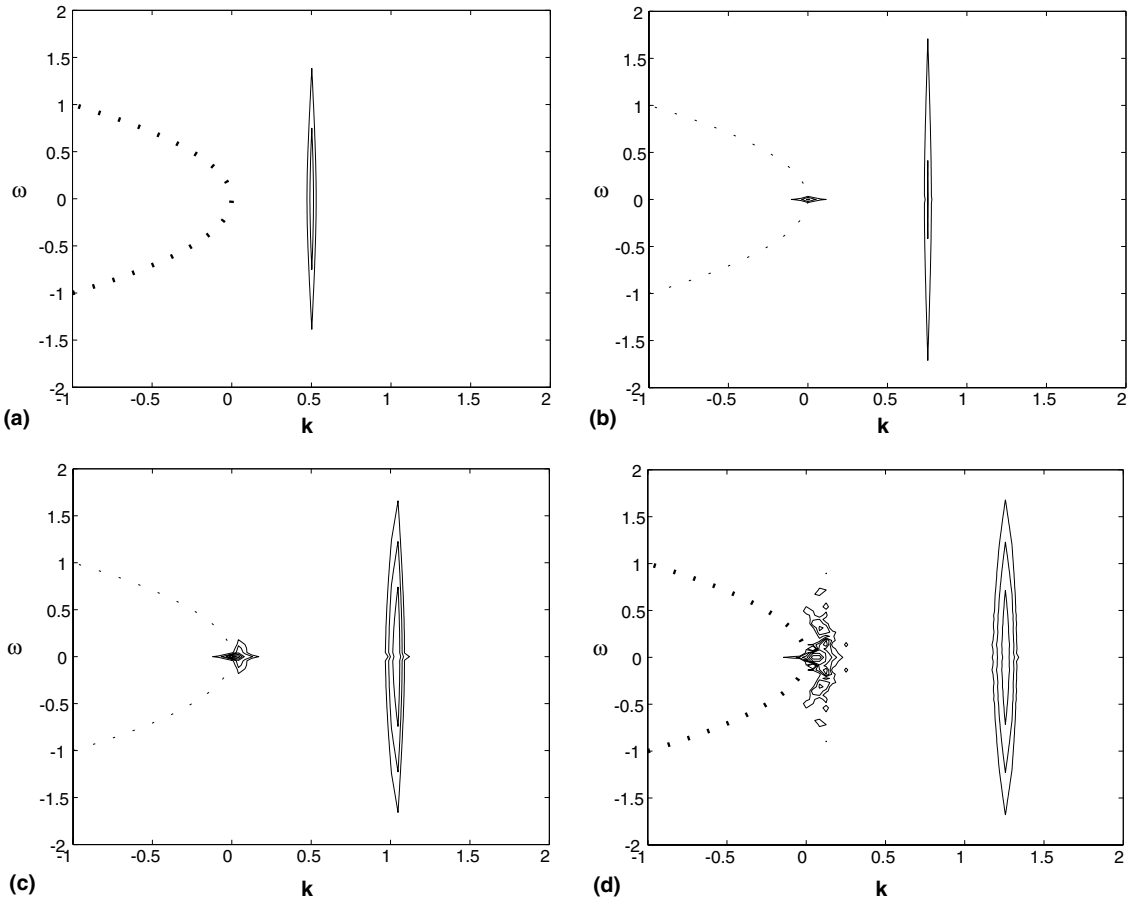

Fig. 9. (a–d) Generalized dispersion relation diagrams (ω, k), as obtained from contour plots of the 2D DFT for pulse propagation under interaction with a CW having $\phi = 0$ and $\alpha = 0,\ 0.08,\ 0.16,\ 0.24$, respectively. The soliton wavenumber shift is shown. The dotted curve (parabola) denotes the dispersion relation of the linearized NLS equation.

some soliton pulse parameters such as mean and peak values of pulse amplitude and spatial frequency of shape and chirp oscillations as shown in Figs. 6(a) and (b) and 7(b) and for the larger CW amplitudes when $\Delta\phi_0 = 0$.

In terms of linear stability analysis [7] the superposition of a waveform on a CW background results in gain for all frequencies of the waveform Ω such that $|\Omega| < 2\alpha$, where α is the CW amplitude. The gain is maximum at $\Omega_{\max} = \pm\alpha\sqrt{2}$ with a peak value $g_{\max} = 2\alpha^2$. The effect of modulational instability pulse interaction with a CW having $\alpha = 0.3$ and $\phi = \pi/2$ is shown in Fig. 8 where the actual period of the pulse train is close to the one obtained from the previous analysis $T = 2\pi/\Omega_{\max}$.

In order to provide an overall visualization of all the spectral components, including pulse, CW and MI, taking part in soliton interactions with CW we utilize a 2D discrete Fourier transform (DFT) of the numerically obtained solutions. The fast Fourier transform (FFT) algorithm is applied along the Z and T dimensions in order to provide the full linear spectral analysis of the solutions in terms of wavenumber k and frequency ω. As a result, all the time-spectral components ω of the initial condition $u(T,0)$ are associated with corresponding wavenumbers k in the sense of a generalized dispersion relation. The contour plot of the 2D spectrum for the case of a soliton without the presence of a CW is shown in Fig. 9(a). The non-linear response of the propagation medium is manifested by the fact that all frequencies ω consisting the soliton sech profile propagate with the same wavenumber $k = 1/2$ as predicted theoretically (Eq. (2)). Figs. 9(b)–(d) show the $\omega - k$ contour plot for the case of soliton interaction with a CW with amplitude $\alpha = 0.08,\ 0.16,\ 0.24$ and phase difference $\Delta\phi_0 = 0$, respectively. The non-soliton part of the initial condition consists of the CW having $(\omega = 0,\ k = 0)$, and the periodic pulse train induced by the modulational instability when present (Fig. 9(d)). As long as the non-soliton part has small amplitude the corresponding ω and k satisfy the dispersion relation $k = -(1/2)\omega^2$ of the linearized NLS equation and each spectral component ω propagates with negative wavenumber. It is remarkable that due to the presence of the soliton pulse and as the amplitude of the CW increases the (ω, k) contours are shifted towards positive k's with respect to the linear dispersion relation. On the other hand the positive wavenumber of the soliton part of the initial condition increases with CW amplitude since the soliton "captures" some of the CW energy. The soliton wavenumber as a function of CW amplitude for $\Delta\phi_0 = 0$ and $\Delta\phi_0 = \pi/2$ is given in Fig. 10. Comparison of soliton amplitude mean values $\langle n\rangle$ given in Fig. 6(a) with the corresponding wavenumbers in Fig. 10 results to the conclusion that for small CW amplitudes $(\alpha \leqslant 0.12)$ the relation $k = (1/2)\langle n\rangle^2$ is satisfied while for larger CW amplitudes $(\alpha \geqslant 0.12)$, $k > 1/2\langle n\rangle^2$.

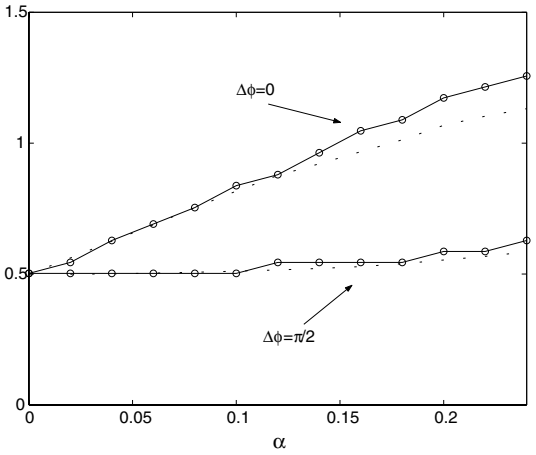

Fig. 10. Soliton wavenumber shift versus CW amplitude for $\phi = 0$ (solid line) and $\phi = \pi/2$ (dashed line). The dotted curve denotes the quantity $1/2\langle n\rangle^2$.

4. Conclusions

Soliton interactions with CW have been considered utilizing a perturbation method which results in a simple model for pulse shape oscillations. According to this model, two distinct types of pulse evolution were predicted, namely oscillatory propagation and pulse destruction, for two different regions of the phase space. Systematic numerical simulations of the NLS equation allowed for the qualitative and quantitative verification of the simple model. The existence of two distinct types of pulse evolution was confirmed and the

frequencies of the oscillations were shown to be predicted in a satisfactory agreement, while the amplitudes were overestimated due to the drastic reduction of the original infinite-degree of freedom system to the one-degree of freedom model. Moreover, numerical simulations were used in order to consider an additional pulse characteristic (thus, an additional degree of freedom), namely the chirp, which was shown to undergo oscillations with the same period with the shape oscillations, and to incorporate the effect of the modulational instability appearing for higher values of CW amplitude. Also, a 2D spectral analysis was proposed as a tool for simple visualization of all the spectral components of the interactions in terms of frequency-wavenumber diagrams in the sense of a generalized dispersion relation. The latter can be used as a tool in order to design the effective filtering and suppression of specific undesirable components of the total spectral content emerging from the interaction.

The fact that the presence of a CW has been shown capable of affecting certain soliton parameters such as amplitude, chirp and wavenumber, suggests that the intentional injection of appropriate CW can act as an all-optical control mechanism of soliton propagation. Considering possible applications, shape oscillations can be utilized for pulse compression, while dynamic prechirping of the pulse can also be accomplished, in all-optical devices based on soliton interactions with CW. This is the subject of present and future work.

Acknowledgements

This research was supported by the ''Archimedes'' and ''Irakleitos'' Research Funds of NTUA/ICCS and the Ministry of Education, respectively.

References

[1] A. Hasegawa, Y. Kodama, Solitons in Optical Communications, Clarendon Press, Oxford, 1995.
[2] W.H. Loh, A.B. Gradinin, V.V. Afanajev, D.N. Payne, Opt. Lett. 19 (1994) 698.
[3] A. Hasegawa, Y. Kodama, Opt. Lett. 7 (1982) 285.
[4] N.N. Akhmediev, S. Wabnitz, J. Opt. Soc. Am. B 9 (1992) 236.
[5] L. Gagnon, J. Opt. Soc. Am. B 10 (1993) 469.
[6] N. Bélanger, P.-A. Bélanger, Opt. Commun. 124 (1996) 301.
[7] G.P. Agrawal, Nonlinear Fiber Optics, third ed., Academic Press, New York, 2001.
[8] R. Avagyan, A. Daryan, S. Dashyan, D. Hovhannisyan, Z. Kalayjian, D. Meghavoryan, K. Stepanyan, Opt. Commun. 203 (2002) 371.
[9] J.P. Gordon, J. Opt. Soc. Am. B 9 (1992) 91.
[10] W.L. Kath, N.F. Smyth, Phys. Rev. E 51 (2) (1995) 1484.
[11] N.F. Smyth, Opt. Commun. 175 (2000) 469.